Relationship between hourly extreme precipitation and local air temperature in the United States

Vimal Mishra,[1] John M. Wallace,[2] and Dennis P. Lettenmaier[1]

Received 18 June 2012; revised 26 June 2012; accepted 28 June 2012; published 25 August 2012.

[1] We examine the relationship between hourly extreme precipitation and daily mean temperature across the Contiguous United States (CONUS) during the period 1950–2009. Logarithmically-transformed hourly extreme precipitation generally increases approximately linearly with the daily mean temperature. At most (about 80%) of the stations, regression slopes between hourly extreme precipitation and daily mean temperature are higher than 7%, the approximate Clausius-Clapyron rate. Stations located in the western coastal region exhibit the lowest regression slopes, with median regression slopes less than 7%, while stations in the northern tier of the CONUS showed higher regression slopes, with median regression slope of 16%. More stations (75%) exhibit regression slopes higher than 7% in summer than in winter (65%). Stations in the southern U.S. have higher regression slopes in winter than in summer, whereas stations in the northern U.S. have higher slopes in summer. It seems physically implausible that the intensity of extreme rainfall events could be as sensitive to local temperature as reflected by the regression slopes. Hence, these large values at least partially may be a consequence of factors relating to temperature gradients as opposed to temperature in its own right. **Citation:** Mishra, V., J. M. Wallace, and D. P. Lettenmaier (2012), Relationship between hourly extreme precipitation and local air temperature in the United States, *Geophys. Res. Lett.*, *39*, L16403, doi:10.1029/2012GL052790.

1. Introduction

[2] Extreme precipitation events are responsible for flooding and landslides, which can cause loss of life and economic damage. Both observational [*Allen and Ingram*, 2002; *Lenderink and van Meijgaard*, 2008; *Liu et al.*, 2009; *Min et al.*, 2011; *Sun et al.*, 2007] and climate model simulations [*Kharin et al.*, 2007; *Gutowski et al.*, 2007; *Meehl et al.*, 2000] show that extreme precipitation events increase as the atmosphere warms. The primary mechanism is increased atmospheric water vapor content at warmer temperatures (Clauisus-Clapeyron control) [*Allen and Ingram*, 2002; *Trenberth et al.*, 2003]. *Min et al.* [2011] argued that human-induced increases in greenhouse gases contribute to the observed intensification of heavy precipitation events over the majority of the Northern Hemisphere's land areas. Furthermore, *Pall et al.* [2011] found that the risk of floods in England and Wales has increased due to anthropogenic warming.

[3] The relationship between air temperature (hereafter "temperature" means surface air temperature unless otherwise indicated) and extreme precipitation events may vary with precipitation durations (hourly, daily, and multi-day). Previous studies [*Allen and Ingram*, 2002; *O'Gorman and Schneider*, 2009; *Pall et al.*, 2007; *Shaw et al.*, 2011] reported that daily extreme precipitation increases at about the Clausis-Clapeyron (CC) rate of around 7% per degree C. However, *Lenderink and van Meijgaard* [2008] found that hourly extreme precipitation events increase at about twice (∼14%) the CC rate when daily mean temperature exceeds 12°C. *Utsumi et al.* [2011] reported, using observations in Japan, that sub-daily scale extreme precipitation events are more sensitive to atmospheric warming than are daily extremes. *Shaw et al.* [2011] analyzed hourly precipitation data at 14 stations and found that in most of the regions they studied, hourly extreme precipitation events follow the CC relationship, at least approximately.

[4] The relationship between sub-daily extreme precipitation events and air temperature may have hydrologic implications for small, rapidly responding catchments such as in urban areas. Urban areas have a large fraction of built (impervious) surface, and short-duration extreme precipitation events can lead to urban flooding. Understanding of the relationship between hourly and sub-daily extreme precipitation events and temperature is vital to provide insights into the nature of changes in extreme precipitation events in urban areas and small catchments that may be associated with climate warming. Despite the importance of hourly extreme precipitation events (especially for flooding), attempts to understand their linkage with temperature have been limited to date. Here, we examine hourly extreme precipitation events and their relationship with daily mean temperature using long-term observations from stations across the contiguous United States (CONUS).

2. Data and Analysis

[5] We obtained hourly precipitation data (DS3240) from the National Climatic Data Center (NCDC) for the period 1950–2009 for about 6000 stations across the CONUS. We then examined data quality in terms of: (i) number of years with significant missing (more than 10%) data, and (ii) changes in the precision of measurement (from 0.01 inch to 0.1 inch). We finally selected 1029 stations that had less than 10% missing data in any year during the period of record (1950–2009). The precision of measurement was changed at some stations during the period of analysis.

[1]Civil and Environmental Engineering, University of Washington, Seattle, Washington, USA.
[2]Atmospheric Sciences, University of Washington, Seattle, Washington, USA.

Corresponding author: D. P. Lettenmaier, Civil and Environmental Engineering, University of Washington, Box 352700, Seattle, WA 98195-2700, USA. (dennisl@u.washington.edu)

0094-8276/12/2012GL052790

However, we found that changes in the precision of measurement do not affect the relationship between hourly extreme precipitation and daily mean temperature substantially, and we analyzed the entire record at all the selected stations.

[6] We used daily mean temperature in our analysis because long-term hourly temperature observations are less available than precipitation. Also, daily mean temperatures provides a better index of the temperature of the air mass associated with precipitation events as contrasted with boundary layer processes, which are more influenced by sub-daily variations of air temperature [see *Lenderink and van Meijgaard*, 2010; *Shaw et al.*, 2011]. We used gridded daily temperature data at 1/16 degree spatial resolution produced by averaging daily minimum and maximum temperatures from the National Climatic Data Center (NCDC) as described in *Maurer et al.* [2002]. We used gridded temperature data rather than station data to avoid record completeness issues, therefore while the precipitation data were taken from stations, the temperature data were for the 1/16 grid cell closest to the station.

[7] We followed the method of *Lenderink and van Meijgaard* [2010] to understand the relationship between mean daily temperature and hourly extreme precipitation events. A similar methodology has been used in several previous studies [*Hardwick Jones et al.*, 2010; *Shaw et al.*, 2011; *Utsumi et al.*, 2011]. For each location, all hourly wet events (P > 0 mm, defined as a 'wet hour') and corresponding daily mean temperatures were extracted to evaluate the relationships during the period 1950–2009. Precipitation for the wet hours was placed in 20 temperature bins (ordered from lowest to highest) with roughly the same number of wet hours in each. We only considered wet hours with daily mean temperature exceeding 0°C to minimize number of snow events (we tested slightly higher thresholds, and found that they had minimal effect on our results). For each temperature bin, using data for all wet hours, the 99th percentile of hourly precipitation (P99) and mean daily temperature (T) were estimated.

[8] After estimating the 99th percentile of hourly precipitation (P99) and mean daily temperature (T), the logarithm of P99 was regressed onto T (see Figure S1 in the auxiliary material for example).[1] The regression equation for the logarithm of P99 and T was used to estimate the percentage change in P99 and with T. The peak point temperature (temperature at which the P99 maxima occurs, T_{P99}) was estimated as well. We then estimated the percentage change in P99 (dP99) per degree increase in temperature (or regression slope in % hereafter) between T_{P99} (highest temperature) and T_1 (lowest temperature), where T_1 was the mean daily temperature (T) for the first bin.

[9] To understand the relationship between frequency of extreme precipitation events and air temperature, we estimated the ratio of the total number of extreme precipitation events above the 95th percentile to the total number of wet hours in each bin. The ratio was defined as the wet-time fraction (WTF). To understand variations in intensity of precipitation, we estimated the fractional contribution of extreme precipitation events (above 95th percentile) to total precipitation (PFRACT) in each bin. Although the precision of measurement was changed at a few stations during the period of record, this had little effect on the estimates of either WTF or PFRACT.

[10] We analyzed composites of mean sea level pressure (SLP) and air temperature at 850 hPa to diagnose atmospheric conditions during the occurrence of extreme precipitation events at the New York City station (New York City Central Park Station, ID 305801) to understand the role of temperature gradients and SLP on extreme precipitation events typical of the eastern U.S.. The 100 largest hourly precipitation events at the New York City station in winter (December through March) and summer (June through September) for the period 1950–2009 were used as the basis for the analysis. SLP and air temperature (at 850 hPa) four times each day were obtained from the NCEP/NCAR reanalysis for each of the precipitation events, and were averaged to form composite maps. In forming the composites we took into account the fact that station measurements are recorded every hour with reference to local time, whereas the NCEP/NCAR reanalysis are performed at 6-hour increments with reference to Universal Time. Spatial patterns in the composite charts were evaluated separately for winter and summer. The compositing analysis was repeated using data for a few other stations in the eastern U.S. and qualitatively similar results were obtained.

[11] To evaluate the urbanization effect on regression slope between extreme precipitation and daily mean temperature, we used a paired approach (as in *Mishra and Lettenmaier* [2011]) to select urban and nonurban stations based on population density. The gridded population density (1 km spatial resolution) was obtained from the Global Urban-Rural Mapping Project (GURMP v1) for the year 2000 from the CIESIN's web site (http://sedac.ciesin.columbia.edu/gpw/global.jsp, accessed on January 15, 2012). Using the gridded density data, we estimated mean population density for each of the 1029 stations within a 5 km buffer region. The 5 km buffer region around each precipitation station was used to classify stations as urban or nonurban. Stations with population density more (less) than 500 (200) person/km^2 were identified as urban (nonurban) stations. We identified 100 urban stations and for each we identified a paired nonurban station (population density less than 200 person/km^2 within 25 km). This threshold of 25 km was increased up to 125 km for urban stations with no closer non-urban pair. The paired approach minimizes the impacts on temperature sensitivity that may be attributable to other factors related to geographical location or climate. We also used all the stations and associated population densities to identify the urbanization influences using an approach based on bins [*Kishtawal et al.*, 2010], however, we note that this approach does not account for the potentially confounding influence of geographic location.

3. Results

3.1. Temperature Dependence of Hourly Extreme Precipitation Events

[12] Figure 1 shows the distribution of regression slope (dP99 expressed in %), goodness of fit (R^2), and the peak point temperature (T_{P99}) for all stations. Most of the stations in the western coastal United States (WC; box 1 in Figure 1a) have regression slope less than CC (~7%) (Figure 1a). For stations located in the southern U.S. (S_US;

[1]Auxiliary materials are available in the HTML. doi:10.1029/2012GL052790.

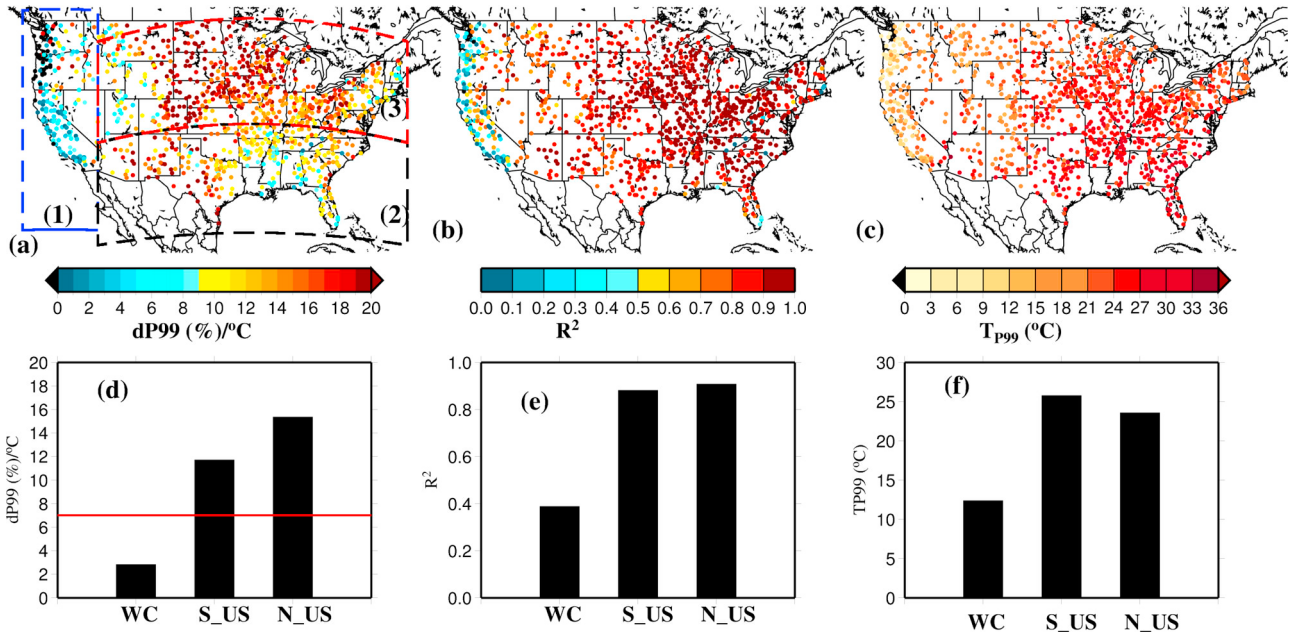

Figure 1. (a) Regression slopes (dP99, %) between hourly extreme precipitation and daily mean temperature for 1029 stations across the United States. The boxes used in panel a) for the west coast (WC) [west of −118° longitude], southern U.S. (S_US) [east of −118° longitude and south of 36° latitude], and northern U.S. (N_US) [east of −118° longitude and north of 36° latitude] are shown as regions 1, 2, and 3, respectively. (b) Coefficient of determination (R^2) estimated using linear regression between log-transformed hourly extreme precipitation and daily mean temperature, (c) peak point temperature (T_{P99}) for the selected sites, (d) median regression slopes (dP99) for locations in the WC, S_US, and N_US regions. The red lines indicate changes (7%/°C) in hourly extreme precipitation events according to the Clausis-Clapeyron (CC) relationship. (e) Median coefficient of determination (R^2), and (f) median peak point temperature (T_{P99}) for locations in WC, S_US, and N_US.

box 2 of Figure 1a), regression slopes vary between 6 and 15%. For instance, stations located in the eastern part of the S_US and in Texas have regression slopes that are higher than CC. The largest regression slopes are for stations located in the northern U.S. (N_US; box 3 of Figure 1a) where most of the locations have slopes greater than CC (Figure 1a). Regression slopes were greater than CC at 83% of the 1029 stations. Regression slopes generally increased with latitude across most of the US.

[13] The goodness of fit between log (P99) and T showed that the linear relationship is robust across the eastern part of the US (Figure 1b). R^2 values exceeded 0.6 for most stations except for those in WC.

[14] Substantial variations in peak point temperature were found across the domain (Figure 1c). For most of the stations in the WC, T_{P99} is below 15°C, as extreme precipitation events occur mostly during the winter season (October to March) in this region. For stations in the S_US and N_US, T_{P99} varies between 20 and 35°C.

[15] We estimated median regression slopes (%) for WC (185 stations), S_US (219 stations), and N_US (625 stations) to understand the regional variability of regression slopes (Figure 1d). The median regression slopes for WC, S_US, and N_US were 2.8, 11.7, and 15.3%, respectively (Figure 1d). Relationships between log (P99) and T were most robust in N_US (R^2 of 0.9, vs. 0.8 for S_US, and 0.4 for WC, see Figure 1e). The median T_{P99} was 14, 26, and 24°C for the WC, S_US, and N_US, respectively (Figure 1f).

3.2. Wet Time Fraction (WTF) and Fractional Contribution by Extreme Precipitation Events (PFRACT)

[16] We estimated WTF and PFRACT in each bin. The relationships between WTF and PFRACT and T for the WC, S_US, and N_US are shown in Figure S2. For locations in the WC, WTF is almost constant with T (Figure S2a). On the other hand, WTF increases rapidly with T for locations in N_US. For locations in S_US, WTF increases rapidly at temperatures below 20°C and at higher temperatures it becomes almost constant. Similar relationships between PFRACT and T were found for WC, S_US, and N_US (Figure S2b). We found that PFRACT increases more rapidly with T than WTF in all the three regions. Thus, it appears that regression slopes between extreme precipitation events and T are more influenced by changes in PFRACT (intensity) than WTF (frequency).

3.3. Regression Slopes in Summer and Winter

[17] Figure 2 shows seasonal variability in regression slopes. In summer, the distribution of regression slopes was somewhat similar to the annual distribution (Figure 2a). For instance, the tendency for larger values at higher latitudes was consistent for annual values and the summer season. Stations located in WC had regression slopes that were mostly less than CC in both summer and winter. However, regression slopes were higher elsewhere, except in the eastern part of S_US (Figure 2a). In summer, median regression slopes were 6.0, 6.4, and 15% for the WC, S_US,

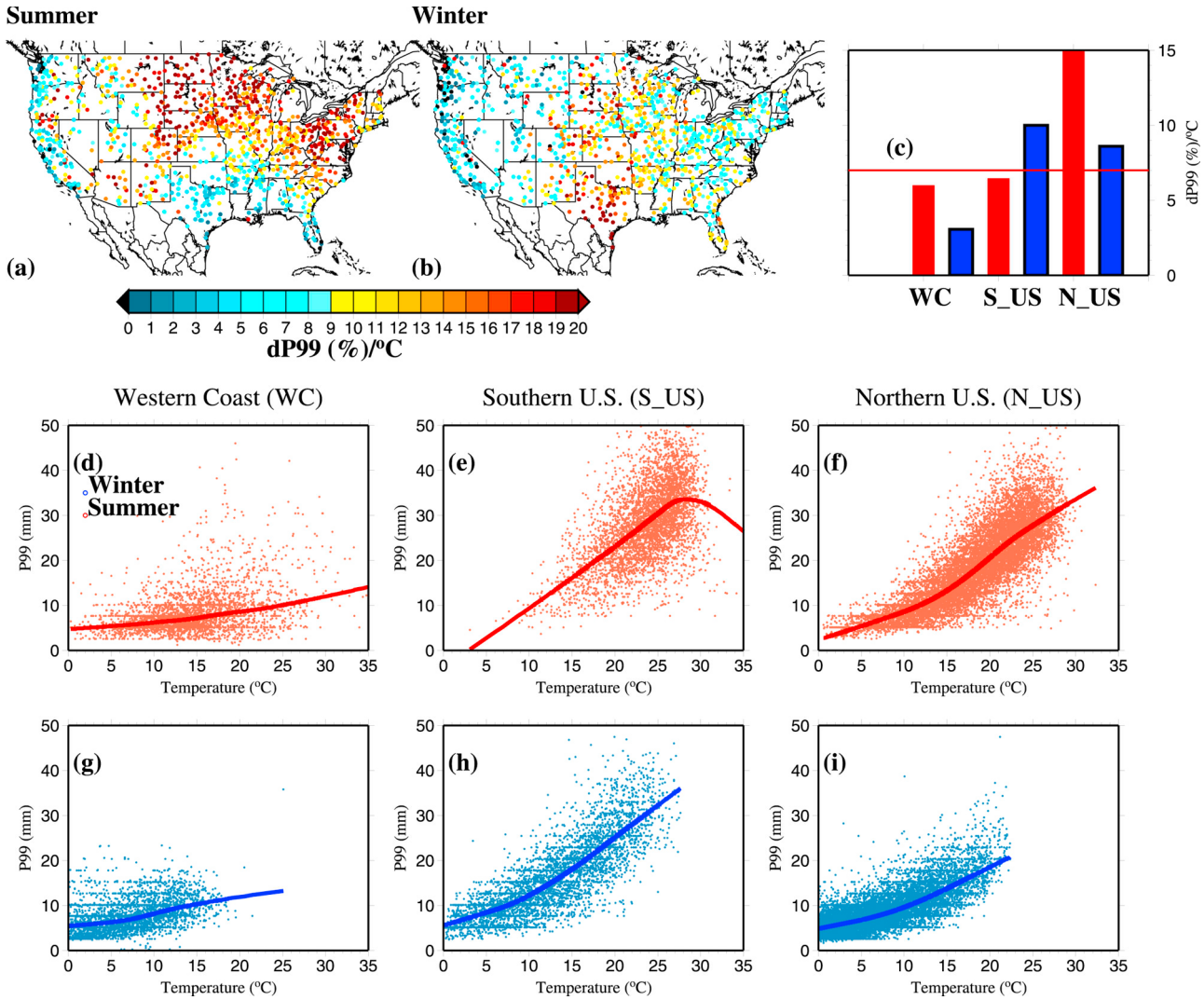

Figure 2. Seasonal distribution of regression slopes (dP99, %) between hourly extreme precipitation and daily mean temperature for: (a) summer (April through September), and (b) winter (October through March). (c) Median regression slopes for the stations in WC, S_US, and N_US (as defined in Figure 1) for summer (red) and winter (blue) seasons. (d–f) Relationship between hourly extreme precipitation events and daily mean temperature in summer for WC, S_US, and N_US, respectively. (g–i) Same as Figures 2d–2f but for winter season. Blue and red lines are the LOWESS curves for winter and summer seasons, respectively. Figures 2d–2i show extreme precipitation and daily mean temperature data in 20 bins at all the stations in the given region. The analysis is based on the hourly precipitation data and daily temperature data for the period 1950–2009.

and N_US, respectively (Figure 2c). In winter, median regression slopes were 3.0, 10.0, 8.6% for the WC, S_US, and N_US, respectively (Figure 2c). In S_US regression slopes were highest in winter, while for N_US, regression slopes were highest in summer (Figures 2a and 2b). Regression slopes exceeded CC at 76 and 65% locations in summer and winter seasons, respectively (Figures 2a and 2b). The distributions of regression slopes for individual sites in WC, S_US, and N_US for the summer and winter seasons (Figures 2d–2i) also showed differences that are apparent in Figures 2a and 2b.

3.4. SLP and Air Temperature (850 hPa) Composites

[18] We constructed composite maps of air temperature anomalies at 850 hPa and mean SLP associated with the 100 most extreme summer and winter precipitation events at the New York City station over the period of record in order to obtain insight into the synoptic settings in which they occur. During the winter (December through March) season positive temperature anomalies of ~3°C are observed over and to the east of New York (40.71°N, 74.0°W) in the composite map (Figure 3a). The associated sea-level pressure pattern for winter events exhibits a low centered over New York with a "V" shaped trough extending to the south, which is the characteristic signature of a cold front. A similar but weaker pattern is observed during summer (Figure 3b). These results are consistent with the conclusion of *Kunkel et al.* [2012] that many of the heaviest rain events over the United States occur in association with the passage of extratropical cyclones and their associated cold fronts.

[19] We used an approach similar to the one described in Section 2 to analyze the relationship between hourly extreme

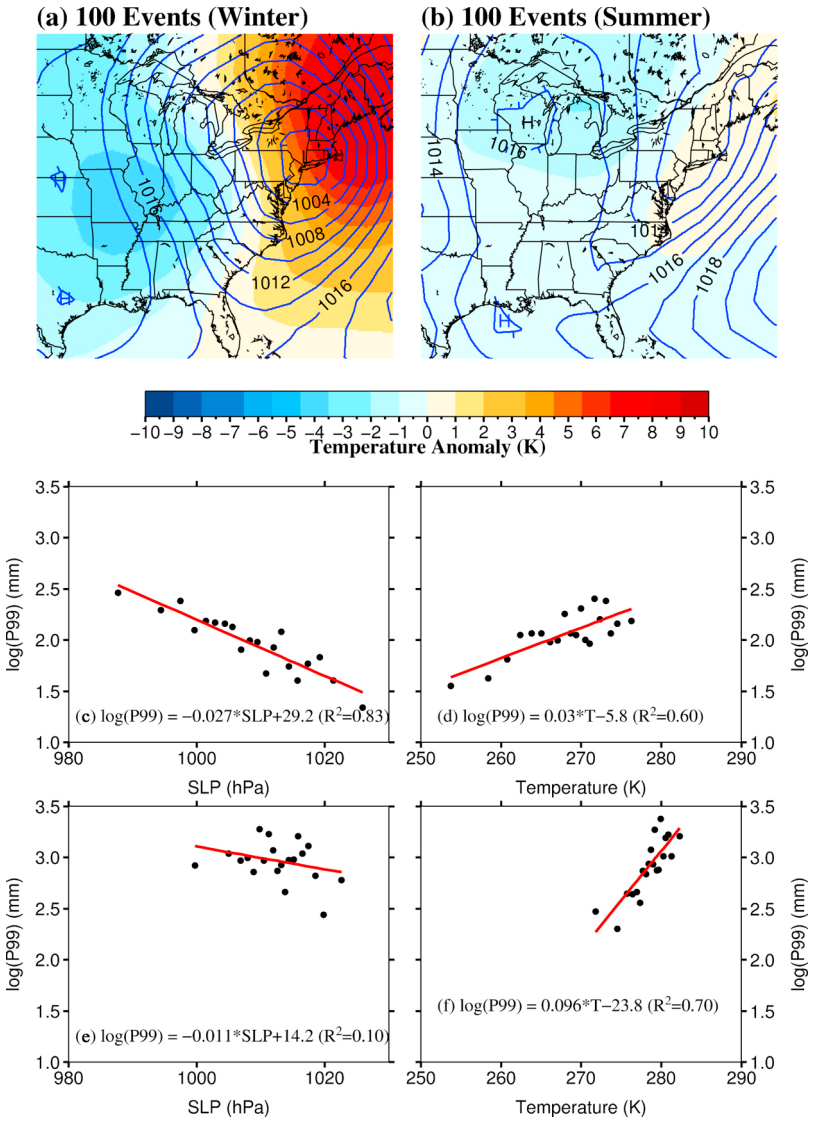

Figure 3. SLP and air temperature anomalies at 850 hPa composites for 100 extreme precipitation events at New York City in (a) winter (December through March), and (b) summer (June through September) seasons. (c) Relationship between log-transformed hourly extreme precipitation (P99) and SLP for winter, (d) same as Figure 3c but for air temperature at 850 hPa. (e, f) Same as Figures 3c and 3d but for summer season. For Figures 3c–3f all wet hours were placed into 20 bins of roughly equal size and 99th percentile of precipitation in each bin and mean SLP/air temperature were estimated.

precipitation events with mean SLP and air temperature at 850 hPa at New York (Figures 3c–3f). All wet hours in the summer and winter seasons were placed into 20 bins in according to SLP and 850 hPa temperature at the time they occurred. During the winter, negative (positive) regression slope between hourly extreme precipitation events and SLP (daily air temperature) was found (Figures 3c and 3d). During the summer, the relationship between hourly extreme precipitation and air temperature was robust, while seal level pressure exhibited a weaker relationship with extreme precipitation (Figures 3e and 3f).

3.5. Regression Slopes for Urban and Nonurban Stations

[20] Figure 4 compares regression slopes for extreme precipitation events (P99) and daily mean temperature (T) for 100 urban and paired nonurban stations. Both urban and paired nonurban stations show geographical variations in regression slopes similar to those in Figures 1 and 2. For instance, regardless of urban or nonurban stations, regression slopes were highest in N_US and lowest in WC (Figures 4a and 4b). Median values of regression slopes were 9.6 and 10.2% for urban and nonurban stations, respectively. The differences in mean regression slopes were not statistically significant (5% level using the two sided Rank Sum test) (Figure 4c). However, the distributions of regression slopes for the 100 urban and paired nonurban stations were found to be significantly different (Figure 4d) based on the two sided Kolmogorov-Smirnov (KS) test – the distribution of slopes was considerably more variable for the urban than the paired nonurban sites.

4. Discussion and Conclusions

[21] We evaluated the relationship between local air temperature and hourly extreme precipitation events for

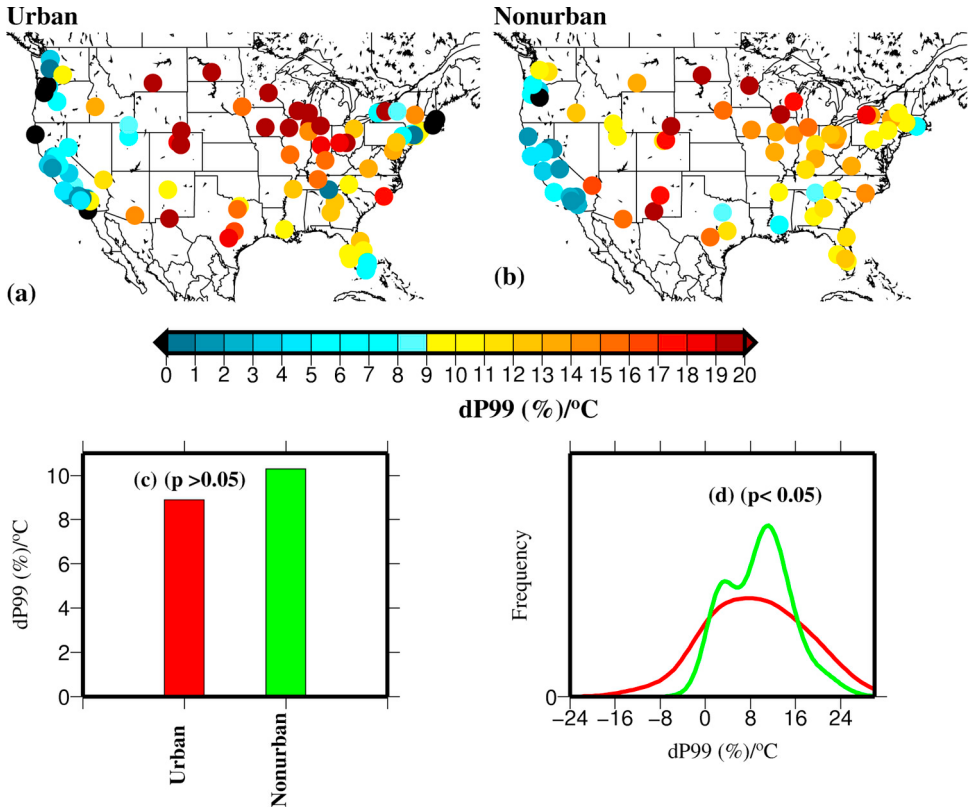

Figure 4. (a, b) Regression slopes (dP99, %) between hourly extreme precipitation and daily mean air temperature for 100 urban and paired nonurban areas, (c) median values of regression slopes for urban and nonurban stations, and (d) kernel density function for regression slopes of urban (red) and nonurban (green) stations estimated using the pooled data. P values (>0.05) in c indicates that mean is not statistically significant at 5% level using the two sided Rank Sum, while in (d) distributions for urban and nonurban areas are significantly different estimated using the KS tests.

1029 stations across the CONUS using hourly precipitation data for the period 1950–2009. Our findings are:

[22] 1. There is a wide range of variability in regression slopes (%) of hourly extreme precipitation events across the CONUS. The WC region had the smallest regression slopes (<CC) between daily mean temperature and the 99th percentile of hourly extreme precipitation events. The median regression slope for stations located in S_US considerably greater than CC (about 10%). The highest regression slopes were for N_US (median > 16%).

[23] 2. WTF and PFRACT increase with air temperature, however, with greater regional variability than in the regression slopes.

[24] 3. Regression slopes in N_US are higher in summer than in winter, whereas in S_US, they are larger in winter than in summer.

[25] 4. Difference in mean regression slopes for urban and non-urban paried stations were not statistically significantly different.

[26] Our results indicate that regression slopes are higher than CC at about 80% of the sites. However, most of these sites are located in northern US and the eastern part of S_US. *Lenderink and van Meijgaard* [2010] reported that hourly extreme precipitation events at De Bilt, Netherland follow a super-CC relationship (about double the CC rate) when daily mean temperature exceeds 12°C. In this respect, our findings are consistent with theirs. While we did not analyze temperature dependence of daily extreme precipitation events, *Utsumi et al.* [2011] in their global analysis found that daily extreme precipitation events in most of the CONUS show sub- CC relationships (slopes less than 5%) (see *Utsumi et al.* [2011, Figure 2b] for details). Therefore, it appears that regression slopes for hourly extreme precipitation events are higher than those for daily extreme precipitation events for most of the U.S.

[27] We found that 75% of the sites had regression slopes greater than CC during the summer, and about 65% in winter. These results suggest that the regression slopes are robust throughout the year. We also found a wide range of spatial variability in the seasonal variations of regression slopes across regions. For instance, in S_US (especially in the Southern Great Plains), regression slopes are higher during winter than in summer. On the other hand, in N_US, regression slopes are higher in summer than in winter. We found a positive relationship between extreme precipitation intensity (P99) and temperature in both seasons across all three regions (Figure 2) but with seasonally varying slopes between P99 and T (Figures 2d–2f). *Berg et al.* [2009] found different regression slopes between extreme precipitation and temperature during the summer and winter seasons in Europe. This spatial and seasonal variability in the regression slopes may be attributable to the type and scale of precipitation as suggested by *Haerter and Berg* [2009] that is often influenced by the synoptic scale circulation pattern (Figure 3).

[28] The nature of precipitation (convective versus large scale) also plays an important role in occurrence and characteristics of extreme precipitation events [*Trenberth et al.*, 2003]. The regression slopes of hourly extreme precipitation events tend to be smaller in WC is probably related to the different properties of the large scale of extreme precipitation events there. Especially in winter, many western U.S. extreme precipitation events are associated with atmospheric rivers that that transport moisture over long distances [*Leung and Qian*, 2009]. Therefore, local variations in temperature are likely to have less effect on extreme precipitation events than temperatures in the moisture source areas, for instance. On the other hand, sites that receive most of their precipitation in the form of convective activity (eastern U.S.) would be expected to have stronger associations with temperature.

[29] Given the physical processes that govern the intensity of precipitation, it seems physically implausible that the intensity of extreme rainfall events could be as sensitive to temperature as indicated by the regression slopes reported here and in papers of *Lenderink and van Meijgaard* [2010], *Utsumi et al.* [2011], and *Hardwick Jones et al.* [2010], many of which are significantly in excess of CC [e.g., see *Held and Soden*, 2006]. Hence it is quite possible that these large values are at least partially a consequence of other factors. For example, it is well established that extreme rainfall events occur mainly rain bands situated within or on the boundary of the warm sector baroclinic waves [e.g., see *Kunkel et al.*, 2012]. Baroclinic waves feed on the available potential energy inherent in the temperature contrasts between warm and cold air masses: the stronger the contrast, the greater the potential for extreme precipitation. Other things being equal, a higher temperature in the warm sector would favor a stronger air mass contrast, more vigorous baroclinic wave development and more intense rain bands. There may be other factors as well that have yet to be considered.

[30] **Acknowledgments.** We gratefully acknowledge the funding for this work from the U.S. Department of Energy (DOE, grant 619642).

[31] The Editor thanks an anonymous reviewer for assisting in the evaluation of this paper.

References

Allen, M. R., and W. J. Ingram (2002), Constraints on future changes in climate and the hydrologic cycle, *Nature*, *419*(6903), 224–232, doi:10.1038/nature01092.

Berg, P., J. O. Haerter, P. Thejll, C. Piani, S. Hagemann, and J. H. Christensen (2009), Seasonal characteristics of the relationship between daily precipitation intensity and surface temperature, *J. Geophys. Res.*, *114*, D18102, doi:10.1029/2009JD012008.

Gutowski, W., Jr., E. Takle, K. Kozak, J. Patton, R. Arritt, and J. Christensen (2007), A possible constraint on regional precipitation intensity changes under global warming, *J. Hydrometeorol.*, *8*(6), 1382–1396, doi:10.1175/2007JHM817.1.

Haerter, J. O., and P. Berg (2009), Unexpected rise in extreme precipitation caused by a shift in rain type?, *Nat. Geosci.*, *2*(6), 372–373, doi:10.1038/ngeo523.

Hardwick Jones, R., S. Westra, and A. Sharma (2010), Observed relationships between extreme sub-daily precipitation, surface temperature, and relative humidity, *Geophys. Res. Lett.*, *37*, L22805, doi:10.1029/2010GL045081.

Held, I. M., and B. J. Soden (2006), Robust responses of the hydrological cycle to global warming, *J. Climate*, *19*, 5686–5699, doi:10.1175/JCLI3990.1.

Kharin, V. V., F. W. Zwiers, X. Zhang, and G. C. Hegerl (2007), Changes in temperature and precipitation extremes in the IPCC ensemble of global coupled model simulations, *J. Clim.*, *20*, 1419–1444, doi:10.1175/JCLI4066.1.

Kishtawal, C. M., D. Niyogi, M. Tewari, R. A. Pielke Sr., and J. M. Shepherd (2010), Urbanization signature in the observed heavy rainfall climatology over India, *Int. J. Climatol.*, *30*(13), 1908–1916, doi:10.1002/joc.2044.

Kunkel, K. E., D. R. Easterling, D. A. R. Kristovich, B. Gleason, L. Stoecker, and R. Smith (2012), Meteorological causes of the secular variations in observed extreme precipitation events for the conterminous United States, *J. Hydrometeorol.*, *13*, 1131–1141, doi:10.1175/JHM-D-11-0108.1.

Lenderink, G., and E. van Meijgaard (2008), Increase in hourly precipitation extremes beyond expectations from temperature changes, *Nat. Geosci.*, *1*(8), 511–514, doi:10.1038/ngeo262.

Lenderink, G., and E. van Meijgaard (2010), Linking increases in hourly precipitation extremes to atmospheric temperature and moisture changes, *Environ. Res. Lett.*, *5*, 025208, doi:10.1088/1748-9326/5/2/025208.

Leung, L. R., and Y. Qian (2009), Atmospheric rivers induced heavy precipitation and flooding in the western U.S. simulated by the WRF regional climate model, *Geophys. Res. Lett.*, *36*, L03820, doi:10.1029/2008GL036445.

Liu, S. C., C. Fu, C.-J. Shiu, J.-P. Chen, and F. Wu (2009), Temperature dependence of global precipitation extremes, *Geophys. Res. Lett.*, *36*, L17702, doi:10.1029/2009GL040218.

Maurer, E., A. Wood, J. Adam, D. Lettenmaier, and B. Nijssen (2002), A long-term hydrologically based dataset of land surface fluxes and states for the conterminous United States, *J. Clim.*, *15*(22), 3237–3251, doi:10.1175/1520-0442(2002)015<3237:ALTHBD>2.0.CO;2.

Meehl, G. A., W. D. Collins, B. A. Boville, J. T. Kiehl, T. Wigley, and J. M. Arblaster (2000), Response of the NCAR Climate System Model to increased CO_2 and the role of physical processes, *J. Clim.*, *13*(11), 1879–1898, doi:10.1175/1520-0442(2000)013<1879:ROTNCS>2.0.CO;2.

Min, S.-K., X. Zhang, F. W. Zwiers, and G. C. Hegerl (2011), Human contribution to more-intense precipitation extremes, *Nature*, *470*(7334), 378–381, doi:10.1038/nature09763.

Mishra, V., and D. P. Lettenmaier (2011), Climatic trends in major U.S. urban areas, 1950–2009, *Geophys. Res. Lett.*, *38*, L16401, doi:10.1029/2011GL048255.

O'Gorman, P. A., and T. Schneider (2009), The physical basis for increases in precipitation extremes in simulations of 21st-century climate change, *Proc. Natl. Acad. Sci. U. S. A.*, *106*(35), 14,773–14,777, doi:10.1073/pnas.0907610106.

Pall, P., M. R. Allen, and D. A. Stone (2007), Testing the Clausius–Clapeyron constraint on changes in extreme precipitation under CO_2 warming, *Clim. Dyn.*, *28*(4), 351–363, doi:10.1007/s00382-006-0180-2.

Pall, P., T. Aina, D. A. Stone, P. A. Stott, T. Nozawa, A. G. J. Hilberts, D. Lohmann, and M. R. Allen (2011), Anthropogenic greenhouse gas contribution to flood risk in England and Wales in autumn 2000, *Nature*, *470*(7334), 382–385, doi:10.1038/nature09762.

Shaw, S. B., A. A. Royem, and S. J. Riha (2011), The relationship between extreme hourly precipitation and surface temperature in different hydroclimatic regions of the United States, *J. Hydrometeorol.*, *12*(2), 319–325, doi:10.1175/2011JHM1364.1.

Sun, Y., S. Solomon, A. Dai, and R. W. Portmann (2007), How often will it rain?, *J. Clim.*, *20*(19), 4801–4818, doi:10.1175/JCLI4263.1.

Trenberth, K. E., A. Dai, R. M. Rasmussen, and D. B. Parsons (2003), The changing character of precipitation, *Bull. Am. Meteorol. Soc.*, *84*(9), 1205–1217, doi:10.1175/BAMS-84-9-1205.

Utsumi, N., S. Seto, S. Kanae, E. E. Maeda, and T. Oki (2011), Does higher surface temperature intensify extreme precipitation?, *Geophys. Res. Lett.*, *38*, L16708, doi:10.1029/2011GL048426.